THE JOURNAL OF BIOLOGICAL CHEMISTRY VOL. 283, NO. 31, pp. 21817–21826, August 1, 2008

Modulation of P-glycoproteins by Auxin Transport Inhibitors Is Mediated by Interaction with Immunophilins*[S]

Received for publication, November 27, 2007, and in revised form, May 19, 2008 Published, JBC Papers in Press, May 22, 2008, DOI 10.1074/jbc.M709655200

Aurélien Bailly[‡], Valpuri Sovero[‡], Vincent Vincenzetti[‡], Diana Santelia[‡1], Dirk Bartnik[§], Bernd W. Koenig[§¶], Stefano Mancuso[‖], Enrico Martinoia[‡], and Markus Geisler[‡2]

From the [‡]Institute of Plant Biology and Zurich-Basel Plant Science Center, University of Zurich, CH-8008 Zurich, Switzerland, the [§]Institute of Neuroscience and Biophysics, Research Centre Jülich, D-52425 Jülich, Germany, the [¶]Institute of Physical Biology, Heinrich-Heine University Düsseldorf, D-40225 Düsseldorf, Germany, and the [‖]Department of Horticulture, University of Firenze, I-50019 Sesto Fiorentino, Italy

The immunophilin-like FKBP42 TWISTED DWARF1 (TWD1) has been shown to control plant development via the positive modulation of ABCB/P-glycoprotein (PGP)-mediated transport of the plant hormone auxin. TWD1 functionally interacts with two closely related proteins, ABCB1/PGP1 and ABCB19/PGP19/MDR1, both of which exhibit the ability to bind to and be inhibited by the synthetic auxin transport inhibitor *N*-1-naphylphtalamic acid (NPA). They are also inhibited by flavonoid compounds, which are suspected modulators of auxin transport. The mechanisms by which flavonoids and NPA interfere with auxin efflux components are unclear. We report here the specific disruption of PGP1-TWD1 interaction by NPA and flavonoids using bioluminescence resonance energy transfer with flavonoids functioning as a classical established inhibitor of mammalian and plant PGPs. Accordingly, TWD1 was shown to mediate modulation of PGP1 efflux activity by these auxin transport inhibitors. NPA bound to both PGP1 and TWD1 but was excluded from the PGP1-TWD1 complex expressed in yeast, suggesting a transient mode of action *in planta*. As a consequence, auxin fluxes and gravitropism in *twd1* roots are less affected by NPA treatment, whereas *TWD1* gain-of-function promotes root bending. Our data support a novel model for the mode of drug-mediated P-glycoprotein regulation mediated via protein-protein interaction with immunophilin-like TWD1.

Bioactive flavonoids derived from plant secondary metabolism serve as important nutraceuticals (1). They have health-promoting effects, including antioxidant, anticarcinogenic, antiviral, and anti-inflammatory activities; however, the cellular targets of the *in vivo* protein remain largely unknown (1, 2). In plants, among other functions, flavonoids such as quercetin, kaempferol, and other aglycone molecules have been shown to inhibit cell-to-cell/polar auxin transport (PAT)[3] and consequently to enhance localized auxin accumulation (1, 3–6). During PAT, the plant hormone auxin, which determines many aspects of plant physiology and development, is moved directionally in a cell-to-cell mode (7–9).

The regulatory impact of flavonoids on PAT initially was based on their ability to compete with N-1-naphtylphtalamic acid (NPA), a synthetic auxin transport inhibitor (ATI) (4, 10–12) and herbicide (naptalam, alanap), for transporter binding sites. This concept is further supported by auxin-related phenotypes of *Arabidopsis* mutants with altered flavonoid levels (1, 3, 13), although fundamental physiological processes occur in the absence of flavonoids. Currently the flavonoids are seen as transport regulators or modulators (14); nevertheless, the mechanisms by which flavonoids interfere with auxin efflux components are not yet clear (1).

The auxin efflux complex is thought to regulate PAT on the molecular level and consists of at least two proteins: a membrane integral transporter and an NPA-binding protein (NBP) regulatory subunit (11, 15–17). Recently, ABCB/P-glycoprotein (PGP)/multidrug resistance (MDR) proteins, members of the expanded *Arabidopsis* ABC (ATP-binding cassette) transporter family (18, 19), have been identified as both auxin transporters (20–24) and high-affinity NBPs (25, 26).

High NPA concentrations cause inhibition of auxin efflux catalyzed by ABCB1/PGP1 and ABCB19/PGP19/MDR1 (20, 21) (hereafter referred to as PGPs), most probably by binding to the transporter itself (26). This is in analogy to flavonoids functioning as inhibitors of plant (20, 21, 24) and mammalian PGPs (2) probably by mimicking ATP and competing for PGP nucleotide-binding domains (27). Overexpression of certain PGPs is associated with increased MDR, whereas loss of function often results in diverse diseases (28) in mammalians.

The immunophilin-like FKBP42, TWISTED DWARF1 (TWD1) (29–31), belongs to the FKBP (FK506-binding protein)-type family of PPIases (peptidyl-prolyl *cis-trans* isomerases, EC

* This work was supported by funds from the Swiss National Fonds (to M. G. and E. M.) and the Novartis Foundation (M. G.). The costs of publication of this article were defrayed in part by the payment of page charges. This article must therefore be hereby marked "*advertisement*" in accordance with 18 U.S.C. Section 1734 solely to indicate this fact.

[S] The on-line version of this article (available at http://www.jbc.org) contains supplemental Experimental Procedures," references, and Figs. S1–S6.

[1] Present address: Zurich-Basel Plant Science Ctr., ETH Zürich Inst. of Plant Science, CH-8092 Zurich, Switzerland.

[2] To whom correspondence should be addressed: University of Zurich, Inst. of Plant Biology and Zurich-Basel Plant Science Ctr., CH-8008 Zurich, Switzerland. Tel.: 41-44-634-8277; Fax: 41-44-634-8204; E-mail: markus.geisler@botinst.uzh.ch.

[3] The abbreviations used are: PAT, polar auxin transport; NPA, *N*-1-naphylphtalamic acid; ATI, auxin transport inhibitor; NBP, NPA-binding protein; PGP, P-glycoprotein; MDR, multidrug resistance; ABC, ATP-binding cassette; FKBP, FK506-binding protein; PPIase, peptidyl-prolyl *cis-trans* isomerase; TWD, Twisted Dwarf; BRET, bioluminescence resonance energy transfer; YFP, yellow fluorescent protein; GFP, green fluorescent protein; CFP, cyan fluorescent protein; IAA, indole-3-acetic acid; BA, benzoic acid; rLuc, *Renilla* luciferase; NBD, nucleotide-binding domain; HA, hemagglutinin.

5.1.2.8) (29, 31, 32). Many but not all PPIases catalyze the *cis-trans* isomerization of *cis*-prolyl bonds and have been identified as targets of immunosuppressant drugs such as FK506 (tacrolimus) (29, 31, 32). The TWD1 C terminus forms a so-called amphipathic in-plane membrane anchor, which probably confers a perpendicular orientation (33) on both the vacuolar (34) and the plasma membrane (30, 35).

TWD1 docks with its N-terminal FK506-binding domain (FKBD), shown to lack PPIase activity and FK506 binding (30, 35), to C-terminal nucleotide-binding domains (18) of PGP1 and PGP19 (see Fig. 1*A*). In this way, TWD1 acts *in planta* as a positive regulator of PGP1- and PGP19-mediated auxin efflux by means of protein-protein interaction (20, 30), modulating the movement of auxin out of apical regions and long range auxin transport on the cellular level (20, 36).

Here, we employed a yeast-based bioluminescence resonance energy transfer (BRET) system to investigate PGP1-TWD1 interaction on a molecular level. Auxin transport inhibitors and flavonoids, inhibitors of mammalian and plant PGPs, disrupt PGP1-TWD1 interaction. Auxin transport inhibitors modulate the regulatory effect of TWD1 on PGP1 activity, supporting a novel mode of PGP regulation via immunophilin-like TWD1 (20). This represents a new concept of drug-mediated ABC transporter modulation via membrane-anchored immunophilins and may have important agronomic and clinical implications.

EXPERIMENTAL PROCEDURES

Yeast Constructs, Growth, and Expression Analysis—cDNA covering the N-terminal FKBD of *Arabidopsis* TWD1 (TWD1-(1–187); At3g21640) were cloned into BamHI and SalI sites of the copper-inducible yeast shuttle vector pRS314CUP (20) resulting in pRS314CUP-FKBD. Point mutations in TWD1 and a stop codon in PGP1 (bp 3.240) were introduced using the QuikChange XL site-directed mutagenesis kit (Stratagene, La Jolla, CA) resulting in pRS314CUP-TWD1^{C70D,L72E} and pNEV-PGP1$^{\Delta NBD2}$-YFP (20). Empty vector controls pNEV and pRS314CUP as well as pNEV-PGP1, pNEV-PGP1-YFP, pNEV-PGP1$^{\Delta NBD2}$-YFP, pRS314CUP-FKBD, pRS314CUP-FKBD-rLuc, pRS314CUP-TWD1, and pRS314CUP-TWD1-rLuc were transformed into *Saccharomyces cerevisiae* strain JK93dα (37), and single colonies were grown in SD-UT (synthetic minimal medium without uracil and tryptophan, supplemented with 2% glucose and 100 μM $CuCl_2$).

Cells co-expressing PGP1-YFP and TWD1-CFP (20) grown in the presence of 10 μM drugs or solvent control to an A_{600} around 0.8 were washed and incubated in mounting media containing 4,6-diamidino-2-phenylindole, and fluorescence pictures were collected by confocal laser scanning microscopy (Leica, DMIRE2) equipped with argon (488 nm) and UV lasers (410 nm). Fluorescence and DIC (differential interference contrast) images were processed using Adobe Photoshop 7.0. Vector controls showed no detectable fluorescence. Plasma membrane fractions were separated via continuous sucrose gradient centrifugation (34) and subjected to 4–20% PAGE (Long Life Gels, Life Therapeutics), and Western blots were immunoprobed using anti-GFP (Roche Applied Science) and anti-*Renilla* luciferase (rLuc; Chemicon Int.).

For auxin analogue detoxification assays (20, 38), transformants grown in SD-UT to an A_{600} of ~0.8 were washed and adjusted to an A_{600} of 1.0 in water. Cells were diluted 10× five times, and each 5 μl was spotted on minimal media plates supplemented with 750 μM 5-fluoroindole (Sigma). Growth at 30 °C was assessed after 3–5 days. Assays were performed with three independent transformants.

BRET Constructs and Assays—*Renilla* luciferase (rLuc, GenBank™ accession number AY189980) was amplified by PCR from plasmid pRL-null (Promega) and inserted in-frame into AscI sites generated in the coding regions of pRS314CUP-FKBD and pRS314CUP-TWD1 (64 bp) using the QuikChange XL site-directed mutagenesis kit (Stratagene). In this way, rLuc was inserted into the very N terminus of TWD1. Single colonies co-expressing PGP1-YFP (20) and TWD1-rLuc were grown in selective synthetic minimal medium (SD-UT) in the presence of inhibitors or adequate amounts of solvents. 200 ml of overnight cultures were harvested at $A_{600} = 1$ by centrifugation for 10 min at 1500 × *g* and washed two times with ice-cold milliQ water. The resulting pellet was suspended in 4 ml of ice-cold lysis buffer (50 mM Tris, 750 mM NaCl, 10 mM EDTA) supplemented with proteases inhibitors (Complete tablets, Roche Diagnostics) and an equivalent volume of acid-washed glass beads (inner diameter, 0.5 mm, Biospec Products Inc.) was added. Cells were broken by vortexing 10 times for 1 min, with 1-min intervals on ice for cooling. The supernatant was decanted, and the beads were washed four times with 10 ml of ice-cold lysis buffer. Supernatants were centrifuged at 4,500 × *g* (S1) and 12,000 × *g* (S2) for 10 min at 4 °C to remove unbroken cells and other debris. Membranes were collected by centrifugation at 100,000 × *g* (P3) for 1 h at 4 °C. The membrane pellet was homogenized using a pestle in 300 μl of ice-cold STED10 buffer (10% sucrose, 50 mM Tris, 1 mM EDTA, 1 mM dithiothreitol) supplemented with proteases inhibitors to give a suspension of about 3 mg of proteins/ml as measured using the Bradford assay (Bio-Rad). All preparations were stored at −80 °C for subsequent use. *In vitro* measurement of the BRET signal was performed using 200 μl of yeast membrane suspension (~600 μg of proteins) in a white 96-well microplate (OptiPlate-96, PerkinElmer Life Sciences). 5 μM coelenterazine (Biotium Inc.) was added, and sequential light emission acquisition in the 410 ± 80 nm and 515 ± 30 nm windows was started after 1 min using the Fusion microplate analyzer (PMT = 1100 V, gain = 1, reading time = 1 s; PerkinElmer Life Sciences). BRET ratios were calculated as described (39) as follows: [(emission at 515 ± 30 nm) − (emission at 410 ± 80 nm) × C_f]/(emission at 410 ± 80 nm), where C_f corresponds to (emission at 515 ± 30 nm)/(emission at 410 ± 80 nm) for the rLuc fusion protein expressed alone in the same experimental conditions. The results are the average of 10 readings collected every minute; presented are average values from 6–10 independent experiments with four replicates each.

Yeast Auxin Transport Assays—IAA transport experiments were performed as in (20). In short, *S. cerevisiae* strains JK93dα (37) were grown as described above, loaded with [^{3}H]-IAA (20 Ci/mmol; American Radiolabeled Chemicals Inc.) for 20 min on ice, washed twice with cold water, and resuspended in 15 ml of SD, pH 5.5. 0.5 ml-aliquots were filtered prior to $t = 0$ min

and after 10 min were incubated at 30 °C. PGP1-mediated IAA export is expressed as relative retention of initial (maximal) loading ($t = 0$ min), which is set to 100%. Presented are average values from 6–8 independent experiments with four replicates each.

Drug Binding Assays—Whole yeast NPA binding assays were performed essentially as described previously (26). 10 ml of yeast cultures were grown as described above to an A_{600} of 1, and cells were resuspended in 10 ml of SD, pH 4.5. To 1-ml aliquots (for each experiment four replicates were used) 10 nM [^{3}H]NPA (60 Ci/mmol) and 10 nM [^{14}C]benzoic acid (BA, 58 mCi/mmol; all from American Radiolabeled Chemicals Inc.) were added in the presence and absence of 10 μM NPA (±10 μM BA for competition experiments; 1000-fold excess). Cells were incubated for 1 h at 4 °C under shaking and washed with ice-cold MilliQ water, and the tips of centrifuge tubes including pellets were subjected to scintillation counting. Reported values are the means of specific binding ([^{3}H]NPA bound in the absence of cold NPA (total) minus [^{3}H]NPA bound in the presence of cold NPA (unspecific)) from 4–8 independent experiments with four replicates each.

For PPIase Affi-Gel pulldown assays, 2 mg of the PPIase domain/FKBD of TWD11–180 expressed in *Escherichia coli* and purified as described previously (40) was coupled to 2 ml of Affi-Gel-15 beads (Bio-Rad). 50 μl of Affi-Gel-PPIase or empty Affi-Gel beads (50% slurry) was resuspended in 450 μl of phosphate-buffered saline, pH 7.4, and 5 μl of radiolabeled [7-^{14}C]BA (58 mCi/mmol, 0.1 mCi/ml) and [^{3}H]NPA (60 Ci/mmol, 1 mCi/ml; all from American Radiolabeled Chemicals Inc.), diluted 20× in phosphate-buffered saline was added to four replications of each. After shaking for 1 h at 4 °C, the beads were filtered on nitrocellulose, and the filters washed three times with cold MilliQ water and finally subjected to scintillation counting. Reported values are the means of specific binding ([^{3}H]NPA bound to Affi-Gel-PPIase minus [^{3}H]NPA bound to empty Affi-Gel beads) per 1 μg of coupled protein as measured using the Bradford assay (Bio-Rad). Presented are average values from 4–8 independent experiments with four replicates each.

For microsomes of *Arabidopsis* NPA binding assays, *Arabidopsis* seedlings were grown in liquid cultures, and microsomes were prepared as described elsewhere (34). Four replicates of each 20 μg ($Pro_{CaMV35S}$-TWD1-HA) or 100 μg of protein (wild-type and *twd1*) in STED10 were incubated with 10 nM [^{3}H]NPA (60 Ci/mmol) and 10 nM [^{14}C]BA (58 mCi/mmol) in the presence and absence of 10 μM NPA (±10 μM BA for competition experiments; 1000-fold excess). After 1 h at 4 °C under shaking, membranes were filtered over nitrocellulose filters (MF 0.45 μm, Millipore) and washed three times with cold MilliQ water, and filters were subjected to scintillation counting. Reported values are the means of specific binding ([^{3}H]NPA bound in the absence of cold NPA (total) minus [^{3}H]NPA bound in the presence of cold NPA (unspecific)) from three independent experiments with four replicates each.

Plant Growth Conditions and Quantitative Analysis of Root Gravitropism—*Arabidopsis thaliana* plants were grown as described previously (30). For quantification of gravitropism in the presence of light (Fig. 5*A*, supplemental Fig. S6*A*), wild type, *pgp1* (At2g36910) and *pgp19* (At3g28860), and *pgp1/pgp19* and *twd1* (At3g21640) mutants (all ecotype Wassilewskija (Ws Wt)), seeds were surface sterilized and grown on 0.5× Murashige and Skoog medium, 0.7% phytoagar (Invitrogen) under continuous light conditions in the presence or absence of 5 μM NPA as described previously (20). The angle of root tips from the vertical plane was determined using Photoshop 7.0. (Adobe Systems, Mountain View, CA), and each gravistimulated root was assigned to one of twelve 30° sectors in the circular histograms; the length of each bar represents the percentage of seedlings showing the same direction of root growth. (Figs. 5 and 6, supplemental Fig. S6). Helical wheels were plotted using PolarBar software.

For quantification of root bending rates (Figs. 5*B* and 6, supplemental Fig. S6*B*), 5 dag seedlings, grown vertically on 0.5× strength Murashige and Skoog medium, 0.7% agar, 1% sucrose were transferred for an additional 12 h onto new plates containing 5 μM NPA or the solvent DMSO. Plates were rotated 90° from the vertical for 7–12 h of gravity stimulation in the dark. The angle of root tips from the vertical plane (root curvature) was determined using Photoshop 7.0. (Adobe Systems), and the rate of curvature was calculated as first derivative of root curvature. The number of seedlings for each genotype was between 72 and 96.

Analysis of IAA Responses—Homozygous T4 generations (20) of *A. thaliana* wild-type (ecotypes Ws and Columbia (Col)), *pgp1*, *pgp19*, *pgp1/pgp19*, and *twd1* mutants (all in Ws Wt) expressing the maximal auxin-inducible reporter Pro_{DR5}-GFP (41) were grown vertically for 5 days as described above and analyzed by confocal laser scanning microscopy (Leica, DMIRE2) equipped with an argon laser (488 nm). In some cases, seedlings were transferred for an additional 12 h onto new plates containing 5 μM NPA or the solvent DMSO and gravistimulated for 2 h by turning the plates 90°. For histological signal localization, differential interference contrast and GFP images were merged electronically using Photoshop 7.0 (Adobe Systems).

Recording of Root Apex Auxin Fluxes Using an IAA-specific Microelectrode—A platinum microelectrode was used to monitor IAA fluxes in *Arabidopsis* roots as described previously (20, 42). For measurements, plants were grown in hydroponic cultures and used at 5 days after germination. Differential current from an IAA-selective microelectrode placed 2 μm from the root surface was recorded in the absence and presence of 5 μM NPA. Relative NPA inhibition was calculated by dividing peak influx values (at 200 nm from the root tip) in the absence of NPA by those in the presence.

Data Analysis—Data were analyzed using Prism 4.0b (GraphPad Software, San Diego, CA), and statistical analysis was performed using SPSS 11.0 (SPSS Inc., Chicago). FKBD structure alignment was performed using PyMol 0.99.

RESULTS

Establishment of a Yeast-based PGP1-TWD1 BRET System—Despite the fact that FKBPs are well known subunits and modulators of multiprotein complexes (20, 37, 43), ABC transporter regulation by FKBPs has been reported only for murine MDR3 and *Arabidopsis* PGP1 (20, 30, 34, 37). On the other hand, the

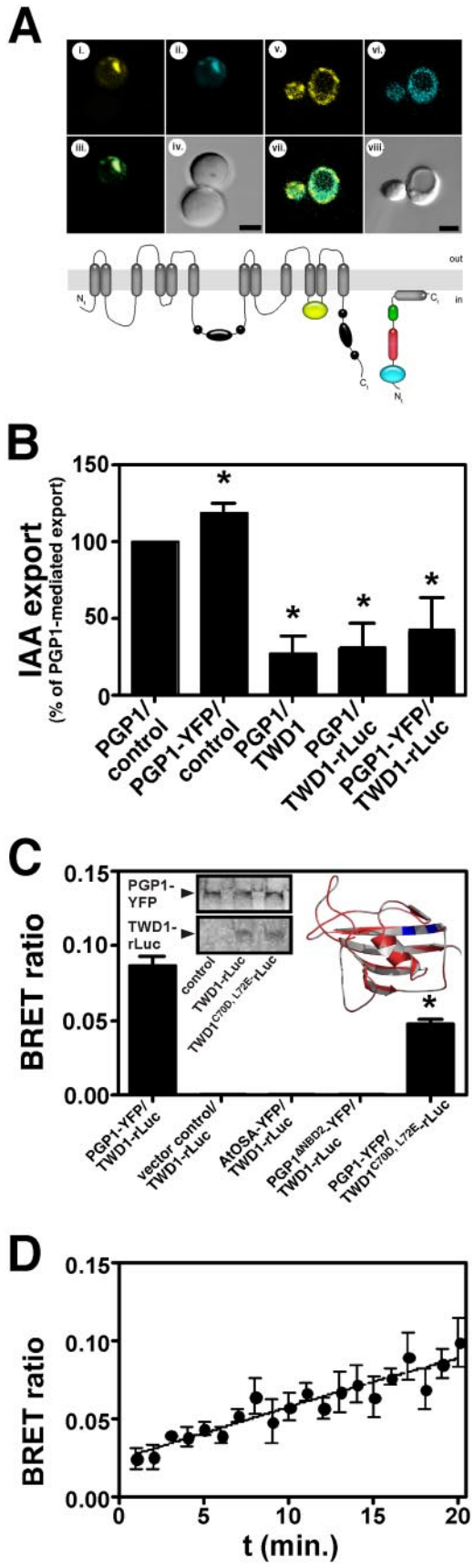

FIGURE 1. **A yeast-based BRET system of TWD1-PGP1 interaction.** *A*, co-localization of PGP1-YFP (*yellow*) and TWD1-CFP (*blue*) in yeast (*upper panels*). The model illustrates PGP1-YFP and TWD1-rLuc interactions resulting in BRET (*lower panels*). *Black*, NBDs; *yellow*, YFP; *red*, FKBD; *green*, tetratricopetide repeat; *blue*, rLuc. The perpendicular orientation of the TWD1 C terminus, forming a so-called amphipatic in-plane membrane anchor, is based on the findings of Scheidt *et al.* (33). *B*, PGP1-YFP and TWD1-rLuc are active. PGP1-YFP exports IAA comparably to native PGP1 (set to 100%), and co-expression of TWD1-rLuc reduces PGP1-mediated IAA efflux to a similar extent as wild type TWD1. Reductions in auxin retention (efflux) were calculated as relative export of initial loading. Data are the means ± S.E. ($n = 4$); means significantly different from native PGP1 control (unpaired *t* test with Welch's correction, $p < 0.05$) are marked by an *asterisk*. *C*, PGP1-YFP-TWD1-rLuc interaction quantified by BRET is specific. PGP1-YFP and TWD1-rLuc were co-expressed in yeast, sequential light emission acquisition on microsomes in 410 ± 80 nm and 515 ± 30 nm windows was quantified, and BRET ratios were calculated as in Angers *et al.* (39). *Inset*, Western detection of PGP1/TWD1 on yeast microsomes (*left*) and structure comparison of native (*red*) and computed TWD1-rLuc$^{C70D,\ L72E}$ (*gray*) (exchanges shown in *blue*) FKBDs (*right*). Data are means ± S.E. ($n = 5$–10); means significantly different from PGP1-YFP/TWD1-rLuc control (unpaired *t* test with Welch's correction, $p < 0.05$) are marked by an *asterisk*. *D*, PGP1-YFP/TWD1-rLuc interaction determined by BRET is stable over time. Presented are means ± S.E. from 6–10 independent experiments with four replicates each.

mechanisms by which NPA or flavonoids interfere with auxin efflux complex components, and hence with PAT (7–9), are not clear (1, 3, 5, 36).

Therefore, and in order to analyze PGP1-TWD1 interaction and its impact on cellular auxin efflux at the molecular level, we established a yeast-based BRET assay by co-expressing TWD1 and PGP1 fused to bioluminescence donor rLuc and acceptor fluorophore YFP, respectively (Fig. 1*A*). In short, BRET is a naturally occurring phenomenon based on the Förster resonance energy transfer between a light-emitting luciferase and an acceptor fluorophore and occurs when the donor and acceptor are below 100 Å apart (44). It has been shown to be independent from substrate concentration and has been validated by its usage in yeast (45) and other cells (39). In summary, BRET offers the advantages of FRET but avoids the drawbacks of fluorescence excitation like photobleaching and direct excitation of the acceptor fluorophore (44).

PGP1-YFP and TWD1-rLuc fusion proteins are functional as shown by analysis of IAA export upon co-expression and PGP1-YFP mediated detoxification of auxin analogs in yeast (Fig. 1*B*, supplemental Fig. S1). Moreover, TWD1-rLuc inhibited PGP1- or PGP1-YFP-mediated auxin efflux to the native TWD1 level. As shown previously, TWD1 has in yeast, unlike in mammalian and plant cells, an inhibitory effect on PGP1 export activity (20, 46). As discussed in detail below (see "Discussion"), the difference might be due to the lack of higher eukaryote components in yeast, the lower abundance of TWD1 *in planta*, or competition of TWD1 with yeast FKBP12 for activation of PGP1.

PGP1-YFP and TWD1-rLuc co-localize on the plasma membrane and small plasma membrane-attached vesicles (Fig. 1, *A* and *C* (20)) and co-expression results in a stable, highly reproducible BRET signal (Fig. 1*C*), which was quantified as a ratio of the light emitted by PGP1-YFP over that emitted by TWD1-rLuc (BRET ratio (39)). This BRET signal was specific because, first, no BRET was observed in the absence of PGP1-YFP (Fig. 1*C*) or with PGP1 minus YFP (not shown) or AtOSA-YFP, an unrelated protein kinase that co-localized with TWD1-CFP (Fig. 1*A*). Second, deletion of the interacting C terminus of PGP1-YFP containing the second nucleotide-binding domain (NBD) (PGP1$^{\Delta NBD2}$-YFP) abolished BRET entirely. And third,

introduction of two point mutations in the β_2 sheet of the TWD1 FKBD (47) (TWD1$^{C70D,\ L72E}$-rLuc), which apparently does not significantly affect the overall FKBD structure and PGP1-YFP expression (Fig. 1*C*, *inset*), reduced BRET significantly (46% reduction; Fig. 1*C*).

Moreover, the specificity of interaction was further validated by the fact that a soluble FKBD-rLuc was specifically retained by PGP1- but not by the related auxin importer, PGP4- (23), or vector control membranes, and a soluble FKBD-rLuc restored BRET when added to PGP1-YFP membranes (supplemental Fig. S2).[4] Together, these results unambiguously demonstrate that PGP1 and TWD1 are compatible partners in yeast and that BRET was specific.

Identification of Drugs That Alter PGP1-TWD1 Interaction Using BRET—BRET signal stability and linearity over time (Fig. 1*D*) allowed us to screen a mini-library of putative ATIs for drugs that were able to alter PGP1-TWD1 interaction. The synthetic ATI, NPA, (4, 10–12) has been shown to bind to *Arabidopsis* PGPs employing whole yeast assays and NPA affinity chromatography (25, 26, 30).

NPA reduced BRET by about 50%, thus disrupting PGP1-TWD1 interaction (Fig. 2*A*). This verifies previous *in planta* data where an excess of NPA was shown to exclude TWD1 from PGP-positive NPA chromatography fractions (30). Not unexpectedly, the ATIs 2,3,5-triiodobenzoic acid (TIBA) and 2-carboxylphenyl-3-phenylpropan-1,3-dione (CPD), known to employ a different locus and mode of action than NPA (17, 48), respectively, did not alter BRET significantly.

Next, we tested representative flavonoids that are known inhibitors of PAT on one hand and of plant (20, 21, 24) and mammalian PGPs (2) on the other. Interestingly, the flavonol quercetin abolished BRET efficiently with an apparent IC_{50} of ~200 nM (Fig. 2*B*). With the exception of the flavonoid precursor chalcone, all flavonoids tested disrupted PGP1-TWD1 interaction but were less efficient than quercetin. Interestingly, quercetin-3-*O*-glucoside and kaempferol-3-*O*-glucoside, the most common *Arabidopsis* flavonol glycoside derivates (5, 13), were as effective as their aglycones in disrupting PGP1-TWD1 interaction. In summary, our data indicate that NPA and flavonoids disrupt TWD1-PGP1 interaction with quercetin being the most efficient.

TWD1 Confers Drug Modulation of PGP1 Efflux Activity—With the intention of investigating the physiological impact of these drugs, we quantified PGP1-mediated IAA transport in the presence of TWD1 in yeast. As shown previously (20, 46) and discussed above and under "Discussion," TWD1 has in yeast, unlike in mammalian and plant cells, an inhibitory effect on PGP1 export activity. NPA and the flavonols quercetin and kaempferol, shown to efficiently disrupt PGP1-TWD1 interaction as monitored by BRET (Fig. 3*A*), therefore, as expected reverted TWD1-mediated inhibition of IAA export catalyzed by PGP1. This resulted in an enhanced IAA export, which is in agreement with a dissociation and hence an activation of the PGP-TWD1 transport complex in yeast. 2,3,5-Triiodobenzoic acid, which is not a representative ATI (48) and which had no significant effect on the TWD1-PGP1 complex (Fig. 2*A*), did not alter IAA transport (Fig. 2*A*).

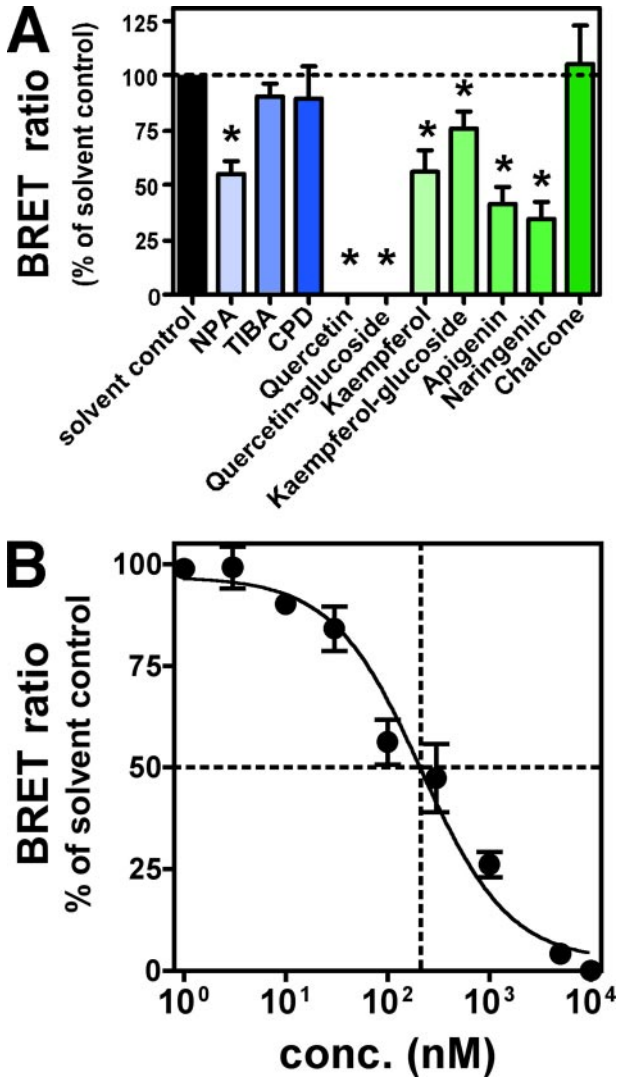

FIGURE 2. **TWD1-PGP1 interaction is disrupted by auxin transport inhibitors.** *A*, PGP1-YFP-TWD1-rLuc interaction quantified by BRET is disrupted by ATI NPA and flavonoids (10 μM). Data are means ± S.E. (n = 6–10); means significantly different from solvent control (unpaired t test with Welch's correction, $p < 0.05$) are marked by an *asterisk*. *B*, dose dependence of complex disruption by the flavonol quercetin. PGP1-YFP and TWD1-rLuc were co-expressed in yeast, sequential light emission acquisition on microsomes in 410 ± 80 nm and 515 ± 30 nm windows was quantified, and BRET ratios were calculated as in Angers *et al.* (39). Presented are the means of BRET ratios ± S.E. (n = 6–10).

This modulatory effect was dependent on TWD1 because drug treatments in the absence of TWD1 had no stimulating and only mildly inhibitory effects (Fig. 3*A*) as reported recently (20, 21). Indirect effects, like mistargeting or altered PGP1 expression caused by drug treatments, were excluded by co-immunolocalization (supplemental Fig. S3) and Western blotting analysis (results not shown) of yeast co-expressing TWD1-CFP and PGP1-YFP.

Point mutations in the FKBD, bisecting the PGP1-TWD1 interaction (Fig. 1*C*), completely abolished transduction of the regulatory effects of quercetin on PGP1 activity (Fig. 3*B*). Moreover, the soluble FKBD of TWD1 alone was sufficient to functionally substitute full-length TWD1 in both PGP1 repression

[4] Direct measurement of PGP1-YFP/FKBD-rLuc BRET was not possible because of the high FKBD-rLuc expression and its strong light emission.

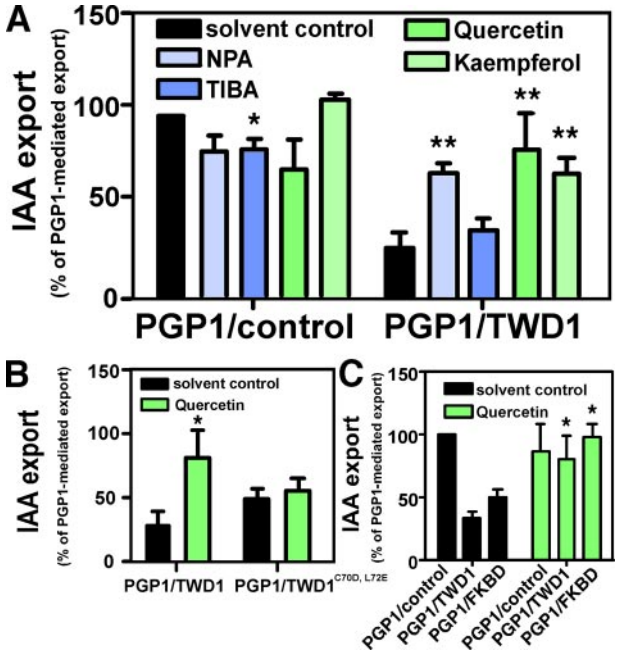

FIGURE 3. **TWD1 confers ATI modulation of PGP1-mediated auxin efflux activity.** *A*, effect of TWD1 on PGP1-mediated IAA export (20) assayed in the presence of auxin transport inhibitors. Data are means ± S.E. ($n = 4–6$). Reductions in auxin retention (efflux) were determined as relative retention of initial loading; PGP1-mediated IAA export was set to 100%. Data are means ± S.E. ($n = 4–6$). *Single asterisks*, significantly different from PGP-mediated IAA transport; *double asterisks*, significantly different from PGP/TWD1-mediated IAA transport. (unpaired *t* test with Welch's correction, $p < 0.05$). *TIBA*, 2,3,5-triiodobenzoic acid . *B*, two point mutations in TWD1-rLuc$^{C70D, L72E}$ abolish the modulatory effect of quercetin on PGP1 activity. Data are means ± S.E. ($n = 4–6$). Reductions in auxin retention (efflux) were determined as relative retention of initial loading; PGP1-mediated IAA export was set to 100%. Data are means ± S.E. ($n = 4–6$); means significantly different from solvent control (unpaired *t* test with Welch's correction, $p < 0.05$) are marked by *asterisks*. *C*, the FKBD of TWD1 is responsible for PGP1 regulation. Co-expression of the soluble FKBD of TWD1 reduces PGP1-mediated IAA efflux to a similar extent as membrane-bound, full-length TWD1. Quercetin (10 μM) disrupts the inhibitory effect of TWD1 and FKBD on PGP1 activity. Data are means ± S.E. ($n = 4–6$); means significantly different from solvent control (unpaired *t* test with Welch's correction, $p < 0.05$) are marked by an *asterisk*.

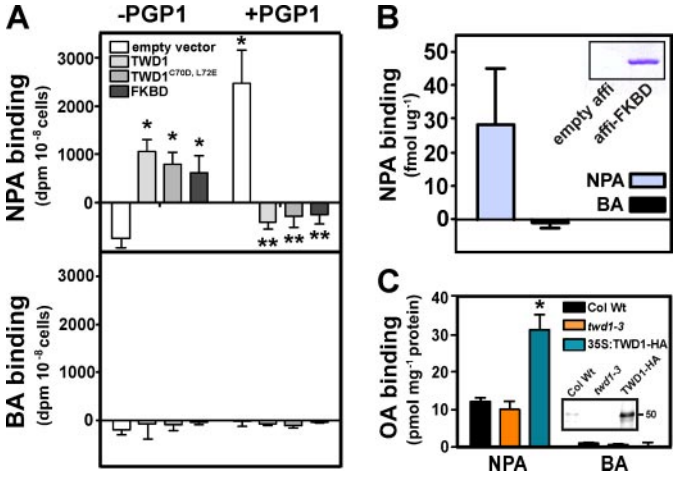

FIGURE 4. **PGP1 and TWD1, but not the PGP1-TWD1 complex, bind NPA.** *A*, binding assays of whole yeast expressing TWD1 and PGP1 assay NPA and BA in parallel. Reported values are means ± S.E. of specific binding from 4–8 independent experiments with four replicates each. *, significantly different from empty vector control; **, significantly different from PGP1 control (unpaired *t* test with Welch's correction, $p < 0.05$). *B*, NPA binding assay using purified Affi-Gel-coupled TWD1 FKBD (PPIase Affi-Gel pulldown assays). Reported values are means of specific binding ± S.E. ($n = 4–6$). *Inset*, Coomassie stain of coupled FKBD. *C*, binding of organic acids (*OA*), NPA and BA (to microsomal fractions of *twd1* and Pro$_{CaMV35S}$-TWD1-HA *35S*.TWD1-HA). Data are means of specific binding ± S.E. ($n = 4$). *Inset*, Western detection of TWD1 from microsomes (each 10 μg of protein). Data are means ± S.E. ($n = 4$); means significantly different from wild type (Col Wt) control (unpaired *t* test with Welch's correction, $p < 0.05$) are marked by an *asterisk*.

and quercetin-mediated reversal of PGP1 activity (Fig. 3*C*). These results taken together indicate that TWD1 functions as an associated modulator of PGP1-mediated auxin transport by mediating the regulatory impact of ATIs via its FKBD.

NPA Binding to PGP1 and TWD1 Is Abolished in the PGP1-TWD1 Complex—NPA was shown to inhibit and bind to PGPs (20, 21); however, an excess of NPA was shown to exclude TWD1 from PGP-positive NPA chromatography fractions (30). To test the hypothesis that TWD1 competes for NPA binding on PGP1, we quantified the binding of radiolabeled NPA using established whole yeast assays (26). NPA binding was specific, as it was outcompeted by an excess of NPA (see "Experimental Procedures") but was not displaced by benzoic acid (not shown). Moreover, whole yeast NPA binding assays (WYNBA) are independent from transport events (supplemental Fig. S4).

PGP1-expressing yeast specifically bound NPA (Fig. 4*A*) as was shown previously for the close homolog PGP19 (26). Surprisingly, a lesser but significant NPA binding was also observed for yeast expressing TWD1 or its FKBD (Fig. 4*A*). NPA binding was specific, as neither PGP1 nor TWD1 bound the organic acid BA, commonly used as a negative control in auxin research. Indirect effects, like TWD1-induced NPA binding to yeast endogenous proteins, were excluded by demonstrating NPA binding to highly purified Affi-Gel-immobilized FKBD (Fig. 4*B*), which was used for crystallization studies (47). In agreement, NPA binding was strongly enhanced in microsomal fractions prepared from *TWD1* gain-of-function plants (Pro$_{CaMV35S}$-TWD1-HA; Fig. 4*C*) compared with wild type. *twd1* microsomes showed reduced but not significant differences in NPA binding compared with wild type, most probably because of the low expression level of *TWD1* (Fig. 4*C*, *inset*) (20, 30).

However, co-expression of PGP1 with TWD1 abolished NPA binding to PGP1 and TWD1 (Fig. 4) but did not significantly alter the expression level of the two proteins (Fig. 1*B*), suggesting that the PGP1-TWD1 (FKBD) complex has a lower affinity for NPA or that binding pockets were simply masked. Again, in analogy to auxin transport assays, co-expression of the FKBD eliminated NPA binding to PGP1, indicating that the N-terminal FKBD was sufficient to perform TWD1 function.

TWD1 Mediates Drug Modulation of P-glycoproteins in Vivo—To test our conclusions derived from the yeast model and to substantiate the physiological relevance of the proposed TWD1 function *in planta*, we investigated NPA sensitivity of *twd1* roots in comparison with those of *pgp* plants using three different assays.

First, we quantified the gravitropic responses, a hallmark of auxin-controlled physiological responses, of *twd1* and *pgp* roots in the presence of NPA, known to disrupt gravitropism in the wild type (49). Performing root gravitropism assays in the presence and absence of light (see "Experimental Procedures")

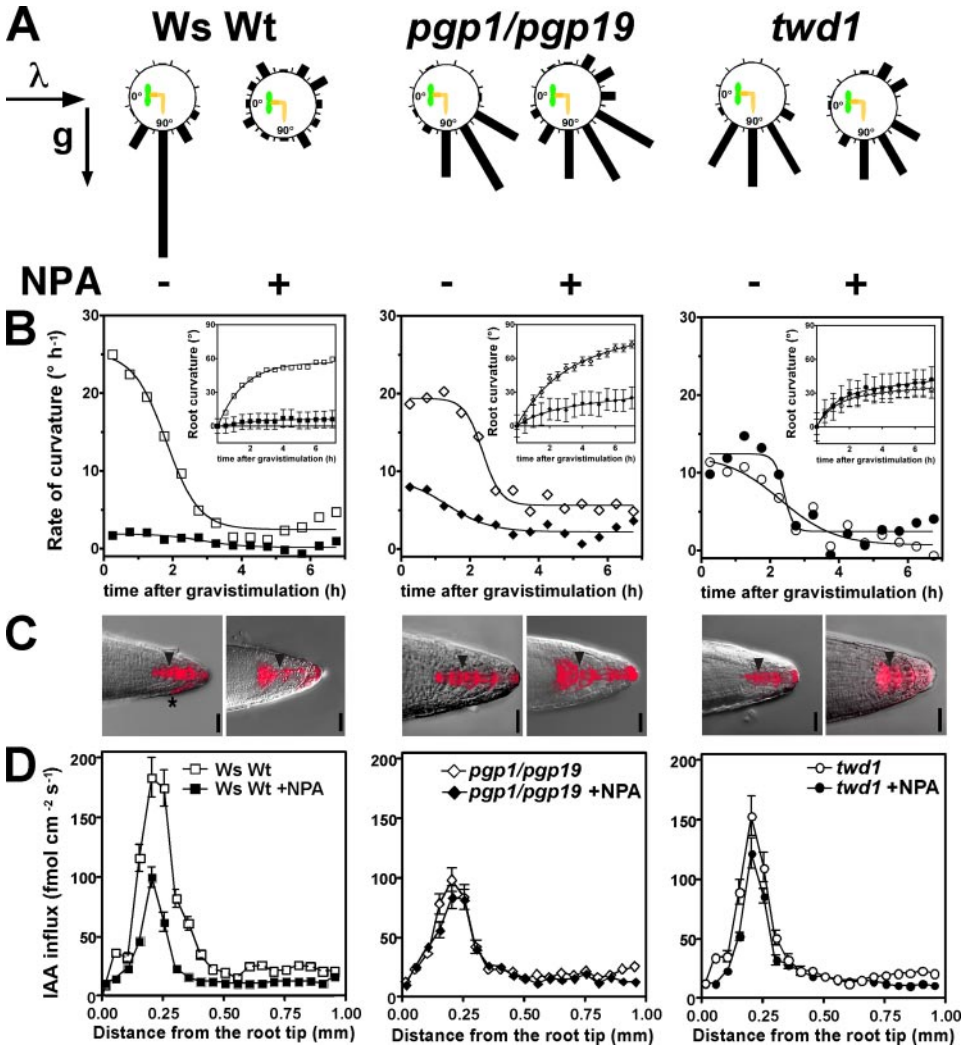

FIGURE 5. **twd1 roots are less sensitive to the auxin transport inhibitor NPA.** *A* and *B*, NPA disrupts gravitropic responses in wild type and, to a lesser extent, in *twd1* roots. Root curvature of *twd1* and *pgp1/pgp19* alleles in comparison with wild type (*Ws Wt*). Seedlings were either grown under continuous light (*A*) as described by Bouchard *et al.* (20) or in the dark (*B*) (see "Experimental Procedures"). Root curvatures were assigned to one of twelve 30° sectors in the *circular histograms*; the length of each *bar* represents the percentage of seedlings showing the same direction of root growth. Data are means ± S.E. ($n = 3$ with each 72–96 seedlings). Shown in *B* is the rate of curvature calculated as first derivative of root curvature (*insets*), with the same description as in *D*. *Arrows* in *A* indicate the direction of light (λ) and gravitropism (*g*). *C*, expression of the auxin-responsive reporter Pro_{DR5}-GFP (20), shown in *red*, upon gravistimulation (from the top). Note that asymmetric auxin accumulation is more pronounced in the commonly used Columbia than in the Wassilewskija ecotype (Fig. S5). *Scale bars*, 200 μm. *D*, IAA influx profile along wild type, *pgp1/pgp19*, and *twd1* roots measured using an IAA-specific microelectrode (20, 23, 42); positive fluxes represent a net IAA influx. Data are means ± S.E. ($n = 6–8$).

revealed that NPA affected *pgp1* and *pgp19* root gravitropism to a similar extent as in the wild type (supplemental Fig. S6). Of special interest was a comparison of *twd1* and *pgp1/pgp19* plants because, based on interaction and transport studies, TWD1 has been proposed to function as a positive modulator of PGP1 and PGP19 auxin transport activities (20, 29, 30, 46). This biochemical evidence is supported by widely overlapping mutant phenotypes (20, 29, 30, 46). Compared with the single *pgp* mutants (supplemental Fig. S6), *pgp1/pgp19* roots were less inhibited by NPA, which was most obvious during the initial, first 3 h of bending (Fig. 5*B*). As shown previously (20, 30), *twd1* showed a more variable and reduced curvature rates compared with the wild type and *pgp* mutants. Interestingly, *twd1* roots were only slightly affected by NPA treatment compared with the solvent control, which is most obvious in the early rates (<3 h) of root curvature (Fig. 5*B*), which were calculated as the first derivative of root curvatures (Fig. 5*B*, *insets*).

Second, asymmetric auxin accumulation along the lower side of the root tip, the primary cause of root bending, was monitored by expression of the auxin-responsive reporter construct Pro_{DR5}-GFP (20, 41) upon gravistimulation. Compared with wild type, basipetal reflux was reduced in *pgp1* but was abolished in *pgp19* (supplemental Fig. S6), *pgp1/pgp19 and twd1* roots (Fig. 3*B*), which is in line with the reported roles for PGP19 and to lesser extent for PGP1 in a coordinated basipetal re-export of auxin out of the root tip (21, 30, 36). However, NPA disrupted basipetal reflux and enhanced the DR5-GFP signal in the quiescent center, the columella initials, the S1 cells in wild type (41), *pgp1*, *pgp19* (supplemental Fig. S6), and *pgp1*/*pgp19* but not in *twd1* roots, which showed instead a faint, diffuse columella DR5-GFP signal (Fig. 5*B*).

Third, we employed an IAA-specific microelectrode that is able to noninvasively record IAA influxes into the root transition zone (20, 23, 42). IAA influx in this zone is characterized by a distinct peak at ~200 μm from the root tip and is consistent with the current auxin "reflux model" (53). *Pgp1*, *pgp19* (supplemental Fig. S6), *pgp1*/*pgp19*, and *twd1* showed reductions of IAA influx compared with wild type (Fig. 3*C* (20, 21)). In agreement with DR5-GFP imaging, relative NPA inhibition of IAA influx was significant in *pgp1* in comparison with wild type but low in *pgp19* and *pgp1/pgp19*. However, NPA had only a negligible inhibitory effect on IAA influx into *twd1* roots (relative inhibition: wild type ≫ *pgp1* > *pgp19* ≅ *pgp1/pgp19* > *twd1*).

To test the impact of TWD1 on PGP-mediated auxin transport in gain-of-function alleles, we measured gravitropic responses of $Pro_{CaMV35S}$-TWD1-HA roots (20). Plants overexpressing TWD1-HA (Fig. 4*C*) perform a more efficient and sharper root curvature compared with wild type and agravitope *twd1–3* (Fig. 6*A*). The kinetics of root bending and rates of curvature clearly indicate that $Pro_{CaMV35S}$-TWD1-HA roots initially bend faster (149%) than those of wild type, whereas *twd1* roots respond more slowly (15%) (Fig. 6*B*). Together,

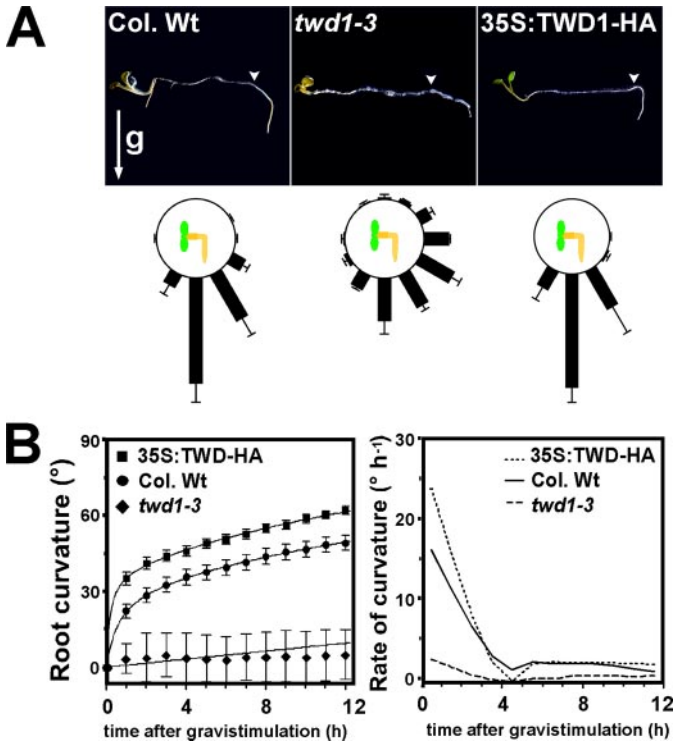

FIGURE 6. **Overexpression of *TWD1* promotes root gravitropism.** *A*, gravitropic root responses of *TWD1* loss- (*twd1–3*) and gain-of-function, $Pro_{CaMV35S}$-TWD1-HA (35S-TWD1-HA) alleles in comparison with wild type (*Col. Wt*). *Triangle* indicates direction of gravitropism (*g*); *triangles* mark time point of 90° plate rotation (*upper panel*). Root curvatures was assigned to one of twelve 30° sectors in the circular histograms; the length of each *bar* represents the percentage of seedlings showing the same direction of root growth. Data are means ± S.E. ($n = 3$ with each 72–96 seedlings). *B*, time series of root curvature (*left panel*) and rate of curvature calculated as first derivative of root curvature (*right panel*).

these data indicate that *TWD1* loss-of-function results in reduced sensitivities to NPA, whereas *TWD1* gain-of-function promotes root gravitropism and NPA binding.

DISCUSSION

Drug Modulation of P-glycoprotein Activity Is Conferred by FKBPs—Previous work has established a role for FKBP42 TWD1 as a positive regulator of PGP-mediated auxin efflux by means of protein-protein interaction (20, 29, 30, 46). Loss of positive regulation of PGP1- and PGP19-mediated auxin efflux activity on the cellular level blocks long range auxin transport *in planta* (20, 36). As a consequence, *PGP1* and *PGP19* single, and more strikingly, double loss-of-function alleles show elevated root auxin levels and defects in root gravitopism (20).

Here, by employing yeast-based, specific TWD1-rLuc/PGP1-YFP BRET and auxin transport systems, we have demonstrated functional disruption of TWD1-PGP1 interaction by NPA and flavonoids, synthetic and *bona fide* native auxin transport inhibitors, respectively. TWD1-PGP1 disruption by NPA is in line with previous findings demonstrating NPA binding to plant PGPs and inhibition of PGP-mediated auxin transport by NPA (20, 23, 24). In contrast to NPA, the ATIs 2,3,5-triiodobenzoic acid and 2-carboxylphenyl-3-phenylpropan-1,3-dione had no significant effect on the TWD1-PGP1 complex stability and auxin transport. This is not unexpected, as 2,3,5-triiodobenzoic acid is structurally unrelated and has been shown to displace NPA binding only partially and even to own weak auxin activity, suggesting a different locus and mode of action compared with NPA (48).

The flavonol quercetin (and its glucose conjugate), of the drugs tested, was the most capable of disrupting TWD1-PGP1. This is of interest because quercetin was the most efficient flavonoid in competing with NPA for auxin transporter binding sites (4). Further, nanomolar IC_{50} values are in agreement with the effective working concentrations of flavonols in blocking PAT (5).[5] Disruption of the TWD1-PGP1 complex by NPA and flavonols leads to activation of auxin transport by the TWD1-PGP1 complex (Figs. 2 and 3), which is reflected by reversal of TWD1-mediated inhibition of PGP1 auxin transport activity. This reversing, inhibitory effect on PGP1 activity in yeast is, as shown previously (20, 23, 24), the opposite of what has been found for mammalian and plant cells. This (reversing, inhibitory) effect or finding either reflects a lack of regulatory components in the lower eukaryotic system (22, 46) or is due to the higher abundance of TWD1 in yeast compared with plant (compare Fig. 1*C versus* Fig. 4*C*) and mammalian cells (20). Therefore, it has been speculated that the TWD1-PGP interaction is of a transient nature *in planta* (20). Alternatively, TWD1 might compete with endogenous yeast FKBP12 for PGP1 binding. scFKBP12 has been shown to activate *Arabidopsis* PGP1 (20) and murine MDR3 (37); assuming enhanced activation of PGP1 by ScFKBP12 but lower affinities to PGP1 compared with TWD1, PGP1-TWD1 co-expression would *de facto* result in an inhibition.

Despite this discrepancy, the disrupting effect of ATIs is in agreement with its proposed inhibitory role in PAT (14). Interestingly, and in opposition to what is seen *in planta,* the inhibitory effect of μM concentration of ATIs on PGP1 expressed alone in yeast is low (around 20–30%), whereas the reversing effect on the TWD1-PGP1 complex is far higher (Fig. 3).

Interaction, transport, and NPA binding studies suggest that the TWD1 FKBD provides the surface for PGP1-TWD1 interaction (21) and is responsible for PGP1 regulation (20, 46) but also confers drug-mediated regulation of PGP1. The soluble FKBD alone can fully complement the full-length, membrane-bound TWD1 in respect to both PGP1 regulation and drug binding and sensing. However, two amino acid exchanges that minimally affect the overall structure and only bisect the interaction (Fig. 1*C*) fully destroy the impact of quercetin on TWD1-PGP1 activity (Fig. 3*B*).

Based on specificity patterns, PGP as a common protein (or protein complex) that mediates hormone efflux as well as hormone action has been proposed (55). Indeed our data support a sensor-like function of TWD1 in PGP regulation by integrating the modulatory impact of flavonoids, the intracellular key signaling molecules of auxin transport and action (1, 7, 9). This concept is sustained by *in planta* data demonstrating reduced NPA sensitivities for TWD1 modulation of root gravitropism and PAT (Fig. 5). Moreover, TWD1 gain-of-function alleles show highly improved initial root-bending performance. These findings together suggest that TWD1 controls PGP-mediated gravisensing by ATIs.

[5] D. Santelia, S. Henrichs, V. Vincenzetti, M. Sauer, L. Bigler, M. Klein, A. Bailly, Y. Lee, J. Friml, M. Geisler, and E. Martinoia, manuscript in preparation.

TWD1 and PGP1 Are Key Components of the NPA-binding Auxin Efflux Complex—NPA binding to PGP1 and TWD1, shown by employing binding studies using either whole yeast, immobilized, highly purified FKBD protein or plant microsomes, respectively is in line with past and recent findings on the regulatory roles of NPA (and flavonoids) on auxin export (7, 10, 14). Until today the identity, number, and affinity of putative NBPs is still controversial (11, 16, 17, 56). But there is apparently a consensus that PIN-formed proteins (57), recently shown to interact functionally with PGPs in auxin transport (58), do not act as NBPs (10). However, our data are in agreement with the broadly accepted current concept that the efflux complex consists of at least two proteins, a transporter and an NPA-binding regulatory subunit (11, 12, 48). Binding to PGP1 (this work and Refs. 25 and 30) and PGP19 (25, 26, 30, 60) support the idea that P-glycoproteins represent the integral, membrane-embedded, NPA-binding proteins identified previously (15, 61). On the other hand, TWD1 might be the peripheral NPB described previously (16), which is in line with the recently proposed perpendicular orientation of the TWD1 C terminus forming a so-called amphipathic in-plane membrane anchor (33). However, this perception is also supported by the fact that the NBP has been suggested to be required for auxin efflux transporter positioning (62). Interestingly, a low-affinity NPA binding site has been associated with the transporter because its block results in transport inhibition, whereas the high-affinity site does not interfere directly with auxin transport (17). However, binding affinities for TWD1 from *Arabidopsis* total microsomes seem to be lower than found for the peripheral NBP from zucchini hypocotyls (16), which might reflect species- and/or tissue-dependent differences in binding affinities.

NPA binding to PGP1 and TWD1 is abolished in the yeast PGP1-TWD1 (FKBD) complex, suggesting that the FKBD apparently competes for NPA binding sites on PGP1. The fact that NPA binding to *pgp* (26, 60) and *twd1* microsomes (60) is reduced compared with the wild type suggests that NPA interrupts transient TWD1-PGP1 interaction *in planta* before they take place and argues against a tight complex as apparently found in yeast. However, individual functional domains on the FKBD are apparently independent, as TWD1$^{C70D,\ L72E}$-rLuc showed reduced affinities to PGP1 (Fig. 1*B*) but was fully capable of blocking NPA binding to PGP1 (Fig. 4*A*). Two more lines of evidence support the identity of more than one NBP: displacement of NPA from microsomes by flavonoids is biphasic (6), but in *Arabidopsis* the membrane-integral NPA-flavonoid interaction site was shown to be associated with PGP1, PGP2, and PGP19, whereas a weaker interaction site correlated with peripheral membrane proteins TWD1 and aminopeptidase APM1 (25). Finally, our data provide a mechanistic explanation for the fact that an excess of NPA during washing steps leads to loss of TWD1 in NPA chromatographies (30). Although the exact role of two individual NBPs remains open (see below), our data provide good evidence that TWD1 and PGP1 represent the high- and low-affinity NPA binding sites, key components of the long sought after NBP auxin transport complex (15, 17, 25).

Flavonoid Modulation of P-glycoprotein-mediated Auxin Transport Conferred by TWD1—Our data highlight the functional importance of the PGP1-TWD1 complex but also support a novel mode of action for ATIs, namely the drug-mediated modulation of transport activity conferred by means of protein-protein interaction. In this scenario, plant endogenous or synthetic ATIs would compete with TWD1 for NPA binding sites on the PGP1 nucleotide binding folds, keeping the TWD1-PGP efflux complex in a dissociated, inactive state, thus allowing flexible fine modulation of activity. However, our data do not unambiguously clarify whether NPA and flavonols employ the same or adjacent, but functionally related, binding sites of a multifaceted ligand binding region (54).

Disruption and inhibition of the TWD1-PGP complex by flavonoids, as supported by our data, is an intriguing option supported by several findings. 1) Lesions in the genes encoding for PGP1 homologs result in reductions in long-distance transport of auxin and consequent dwarfism in mutant plants. These data together with tissue-specific accumulation of flavonols in *Arabidopsis* seedlings that coincide with regions of high auxin levels (5, 6) suggest that flavonols affect polar auxin transport in apical tissues by modulating auxin loading into the long-distance auxin stream (5). Moreover, genetic evidence that flavonoids generally act on PGPs transporting auxin is provided by the epistatic relationship of *pgp4* (*mdr4*, *abcb4*) to the *tt4* phenylpropanoid pathway mutation (36). 2) Aglycone flavonols were localized in a developmentally and tissue-specific manner in the plasma membrane (13, 50) of tissues that strongly overlap with *PGP1* and *PGP19* expression (30, 58). Accordingly, flavonol glucoside contents are drastically altered in *twd1* and *pgp1/pgp19* mutants (results not shown).

Agronomic and Clinical Implications of Drug-mediated ABC Transporter Modulation via Immunophilins—Loss-of *PGP1* gene function has been shown to increase stem diameter in the agriculturally important *brachytic2* and *dwarf3* mutants in maize and sorghum (51). Our yeast-based BRET system will allow rapid and sensitive chemical genetic screens to be performed to identify novel growth promoters or inhibitors that influence plant development and thus plant productivity (agrochemicals) in efforts to confer structural stability to crops.

Moreover, two findings imply that this novel mode of ABC transporter regulation via sensor-like immunophilins might be of interest beyond the plant field. Flavonoids have, as in plants, a modulatory impact on mammalian PGP activity and thus on MDR (27, 52), but the data support both inhibitory and stimulating effects (52). Our findings that inhibitory flavonoid modulation is conferred by interacting FKBPs might explain the conflicting results of flavonoid action, which might be due to tissue-specific immunophilin-PGP complex formation. Moreover, the mammalian TWD1 homolog, FKBP38, is localized to the outer membrane of mitochondria where it helps to anchor the anti-apoptosis proteins Bcl-2 and Bcl-xL (59). Taken together, membrane-anchored FKBPs and their interactive partners might be a promising target for genetic or chemical manipulation for new drug development and disease treatments.

Acknowledgments—We thank Aileen Funke for help with protein purification, Christian Fankhauser for assistance during gravity assays, Sina Henrichs and Shaun Peters for critical comments on the manuscript, Bo Burla for PolarBar software, and Michal Jasinski for the donation of yeast expression plasmid pNEV-AtOSA-YFP (At5g64940). Special thanks go to Rainer Hertel for sharing timely historical information and encouraging discussions.

REFERENCES

1. Taylor, L. P., and Grotewold, E. (2005) *Curr. Opin. Plant Biol.* **8,** 317–323
2. Morris, M. E., and Zhang, S. (2006) *Life Sci.* **78,** 2116–2130
3. Brown, D. E., Rashotte, A. M., Murphy, A. S., Normanly, J., Tague, B. W., Peer, W. A., Taiz, L., and Muday, G. K. (2001) *Plant Physiol.* **126,** 524–535
4. Jacobs, M., and Rubery, P. H. (1988) *Science* **241,** 346–349
5. Peer, W. A., Bandyopadhyay, A., Blakeslee, J. J., Makam, S. N., Chen, R. J., Masson, P. H., and Murphy, A. S. (2004) *Plant Cell* **16,** 1898–1911
6. Murphy, A., Peer, W. A., and Taiz, L. (2000) *Planta* **211,** 315–324
7. Blakeslee, J. J., Peer, W. A., and Murphy, A. S. (2005) *Curr. Opin. Plant Biol.* **8,** 494–500
8. Kerr, I. D., and Bennett, M. J. (2007) *Biochem. J.* **401,** 613–622
9. Vieten, A., Sauer, M., Brewer, P. B., and Friml, J. (2007) *Trends Plant Sci.* **12,** 160–168
10. Lomax, T. L., Muday, G. K., and Rubery, P. H. (1995) in *Plant Hormones: Physiology, Biochemistry and Molecular Biology* (Davies, P. J., ed) pp. 509–530, Kluwer, Dordrecht, Netherlands
11. Luschnig, C. (2001) *Curr. Biol.* **11,** R831–833
12. Morris, D. A. (2000) *Plant Growth Regul.* **32,** 161–172
13. Peer, W. A., Brown, D. E., Tague, B. W., Muday, G. K., Taiz, L., and Murphy, A. S. (2001) *Plant Physiol.* **126,** 536–548
14. Peer, W. A., and Murphy, A. S. (2007) *Trends Plant Sci.* **12,** 556–563
15. Bernasconi, P. (1996) *Physiol. Plant.* **96,** 205–210
16. Cox, D. N., and Muday, G. K. (1994) *Plant Cell* **6,** 1941–1953
17. Michalke, W., Katekar, G. F., and Geissler, A. E. (1992) *Planta* **187,** 254–260
18. Martinoia, E., Klein, M., Geisler, M., Bovet, L., Forestier, C., Kolukisaoglu, U., Muller- Rober, B., and Schulz, B. (2002) *Planta* **214,** 345–355
19. Verrier, P. J., Bird, D., Burla, B., Dassa, E., Forestier, C., Geisler, M., Klein, M., Kolukisaoglu, U., Lee, Y., Martinoia, E., Murphy, A., Rea, P. A., Samuels, L., Schulz, B., Spalding, E. J., Yazaki, K., and Theodoulou, F. L. (2008) *Trends Plant Sci.*
20. Bouchard, R., Bailly, A., Blakeslee, J. J., Oehring, S. C., Vincenzetti, V., Lee, O. R., Paponov, I., Palme, K., Mancuso, S., Murphy, A. S., Schulz, B., and Geisler, M. (2006) *J. Biol. Chem.* **281,** 30603–30612
21. Geisler, M., Blakeslee, J. J., Bouchard, R., Lee, O. R., Vincenzetti, V., Bandyopadhyay, A., Titapiwatanakun, B., Peer, W. A., Bailly, A., Richards, E. L., Ejendal, K. F., Smith, A. P., Baroux, C., Grossniklaus, U., Muller, A., Hrycyna, C. A., Dudler, R., Murphy, A. S., and Martinoia, E. (2005) *Plant J.* **44,** 179–194
22. Geisler, M., and Murphy, A. S. (2006) *FEBS Lett.* **580,** 1094–1102
23. Santelia, D., Vincenzetti, V., Azzarello, E., Bovet, L., Fukao, Y., Duchtig, P., Mancuso, S., Martinoia, E., and Geisler, M. (2005) *FEBS Lett.* **579,** 5399–5406
24. Terasaka, K., Blakeslee, J. J., Titapiwatanakun, B., Peer, W. A., Bandyopadhyay, A., Makam, S. N., Lee, O. R., Richards, E. L., Murphy, A. S., Sato, F., and Yazaki, K. (2005) *Plant Cell* **17,** 2922–2939
25. Murphy, A. S., Hoogner, K. R., Peer, W. A., and Taiz, L. (2002) *Plant Physiol.* **128,** 935–950
26. Noh, B., Murphy, A. S., and Spalding, E. P. (2001) *Plant Cell* **13,** 2441–2454
27. Conseil, G., Baubichon-Cortay, H., Dayan, G., Jault, J. M., Barron, D., and Di Pietro, A. (1998) *Proc. Natl. Acad. Sci. U. S. A.* **95,** 9831–9836
28. Dean, M. (2005) *Methods Enzymol.* **400,** 409–429
29. Geisler, M., and Bailly, A. (2007) *Trends Plant Sci.* **12,** 465–473
30. Geisler, M., Kolukisaoglu, H. U., Bouchard, R., Billion, K., Berger, J., Saal, B., Frangne, N., Koncz-Kalman, Z., Koncz, C., Dudler, R., Blakeslee, J. J., Murphy, A. S., Martinoia, E., and Schulz, B. (2003) *Mol. Biol. Cell* **14,** 4238–4249
31. Romano, P., Gray, J., Horton, P., and Luan, S. (2005) *New Phytol.* **166,** 753–769
32. Fanghanel, J., and Fischer, G. (2004) *Front. Biosci.* **9,** 3453–3478
33. Scheidt, H. A., Vogel, A., Eckhoff, A., Koenig, B. W., and Huster, D. (2007) *Eur. Biophys. J.* **36,** 393–404
34. Geisler, M., Girin, M., Brandt, S., Vincenzetti, V., Plaza, S., Paris, N., Kobae, Y., Maeshima, M., Billion, K., Kolukisaoglu, U. H., Schulz, B., and Martinoia, E. (2004) *Mol. Biol. Cell* **15,** 3393–3405
35. Kamphausen, T., Fanghanel, J., Neumann, D., Schulz, B., and Rahfeld, J. U. (2002) *Plant J.* **32,** 263–276
36. Lewis, D. R., Miller, N. D., Splitt, B. L., Wu, G., and Spalding, E. P. (2007) *Plant Cell* **19**
37. Hemenway, C. S., and Heitman, J. (1996) *J. Biol. Chem.* **271,** 18527–18534
38. Luschnig, C., Gaxiola, R. A., Grisafi, P., and Fink, G. R. (1998) *Genes Dev.* **12,** 2175–2187
39. Angers, S., Salahpour, A., Joly, E., Hilairet, S., Chelsky, D., Dennis, M., and Bouvier, M. (2000) *Proc. Natl. Acad. Sci. U. S. A.* **97,** 3684–3689
40. Weiergraber, O. H., Eckhoff, A., and Granzin, J. (2006) *FEBS Lett.* **580,** 251–255
41. Ottenschlager, I., Wolff, P., Wolverton, C., Bhalerao, R. P., Sandberg, G., Ishikawa, H., Evans, M., and Palme, K. (2003) *Proc. Natl. Acad. Sci. U. S. A.* **100,** 2987–2991
42. Mancuso, S., Marras, A. M., Magnus, V., and Baluska, F. (2005) *Anal. Biochem.* **341,** 344–351
43. Chelu, M. G., Danila, C. I., Gilman, C. P., and Hamilton, S. L. (2004) *Trends Cardiovasc. Med.* **14,** 227–234
44. Xu, Y., Piston, D. W., and Johnson, C. H. (1999) *Proc. Natl. Acad. Sci. U. S. A.* **96,** 151–156
45. Gehret, A. U., Bajaj, A., Naider, F., and Dumont, M. E. (2006) *J. Biol. Chem.* **281,** 20698–20714
46. Bailly, A., Sovero, V., and Geisler, M. (2006) *Plant Signal. Behav.* **1,** 277–280
47. Granzin, J., Eckhoff, A., and Weiergraber, O. H. (2006) *J. Mol. Biol.* **364,** 799–809
48. Petrasek, J., Cerna, A., Schwarzerova, K., Elckner, M., Morris, D. A., and Zazimalova, E. (2003) *Plant Physiol.* **131,** 254–263
49. Rashotte, A. M., Brady, S. R., Reed, R. C., Ante, S. J., and Muday, G. K. (2000) *Plant Physiol.* **122,** 481–490
50. Buer, C. S., Muday, G. K., and Djordjevic, M. A. (2007) *Plant Physiol.*
51. Multani, D. S., Briggs, S. P., Chamberlin, M. A., Blakeslee, J. J., Murphy, A. S., and Johal, G. S. (2003) *Science* **302,** 81–84
52. Zhang, S., Yang, X., Coburn, R. A., and Morris, M. E. (2005) *Biochem. Pharmacol.* **70,** 627–639
53. Blilou, I., Xu, J., Wildwater, M., Willemsen, V., Paponov, I., Friml, J., Heidstra, R., Aida, M., Palme, K., and Scheres, B. (2005) *Nature* **433,** 39–44
54. Brunn, S. A., Muday, G. K., and Haworth, P. (1992) *Plant Physiol.* **98,** 101–107
55. Hossel, D., Schmeiser, C., and Hertel, R. (2005) *Plant Biol.* (*Stuttg*) **7,** 41–48
56. Sussman, M. R., and Gardner, G. (1980) *Plant Physiol.* **66,** 1074–1078
57. Petrasek, J., Mravec, J., Bouchard, R., Blakeslee, J. J., Abas, M., Seifertova, D., Wisniewska, J., Tadele, Z., Kubes, M., Covanova, M., Dhonukshe, P., Skupa, P., Benkova, E., Perry, L., Krecek, P., Lee, O. R., Fink, G. R., Geisler, M., Murphy, A. S., Luschnig, C., Zazimalova, E., and Friml, J. (2006) *Science* **312,** 914–918
58. Blakeslee, J. J., Bandyopadhyay, A., Lee, O. R., Mravec, J., Titapiwatanakun, B., Sauer, M., Makam, S. N., Cheng, Y., Bouchard, R., Adamec, J., Geisler, M., Nagashima, A., Sakai, T., Martinoia, E., Friml, J., Peer, W. A., and Murphy, A. S. (2007) *Plant Cell* **19,** 131–147
59. Shirane, M., and Nakayama, K. I. (2003) *Nat. Cell Biol.* **5,** 28–37
60. Rojas-Pierce, M., Titapiwatanakun, B., Sohn, E. J., Fang, F., Larive, C. K., Blakeslee, J., Cheng, Y., Cutler, S. R., Peer, W. A., Murphy, A. S., and Raikhel, N. V. (2007) *Chem. Biol.* **14,** 1366–1376
61. Ruegger, M., Dewey, E., Hobbie, L., Brown, D., Bernasconi, P., Turner, J., Muday, G., and Estelle, M. (1997) *Plant Cell* **9,** 745–757
62. Gil, P., Dewey, E., Friml, J., Zhao, Y., Snowden, K. C., Putterill, J., Palme, K., Estelle, M., and Chory, J. (2001) *Genes Dev.* **15,** 1985–1997